pol-lutant 3,6-dinitrobenzo[*e*]pyrene in *Salmonella typhimurium* umu strains ex- pressing human cytochrome P450 and *N*- acetyltransferase, Toxicology Letters, 188, 258-262, 2009.

2. 学会発表

1. 穀内修、渡辺徹志 他、大気粉塵の生物活性・化学成分の季節変動及び大陸からの長距離輸送による影響、日本薬学会第130年会、岡山市、2010年3月.
2. 小林沙衣、渡辺徹志 他、新規メイラード反応生成物アミノアゼピノキノリノン誘導体の遺伝子毒性、日本薬学会第130年会、岡山市、2010年3月.

H. 知的財産権の出願・登録状況
（予定を含む。）

1. 特許取得
なし
2. 実用新案登録
なし
3.その他
なし

厚生労働科学研究費補助金(地球規模保健課題推進研究事業（国際医学協力研究事業）)
分担研究報告書

大気中粒子状物質が気道炎症に及ぼす影響に関する疫学的検討

研究分担者　　島　正之　　兵庫医科大学　教授

研究要旨

女子大学生の肺機能検査を２年間にわたって各季節に約２週間ずつ、毎日朝と夜に繰り返し実施した。ピークフロー値及び１秒量は大気中粒子状物質をはじめとする汚染物質濃度との間に有意な負の相関が認められる時期があったが、必ずしも一貫性のある結果ではなかった。全期を通した解析では、アレルギー素因を有する者では大気中二酸化窒素濃度との関連が有意であり、アレルギー素因を有する者は大気汚染物質の影響を受けやすい可能性が示唆された。

A．研究目的

大気中粒子状物質及びオゾン等の大気汚染物質が呼吸器系に与える影響と、それに関連する因子を疫学的に評価することを目的とした。これまで気管支喘息等の呼吸器疾患を有する者では大気汚染物質とアレルギー性気道炎症の増悪との関連が示唆されているが、健常者の呼吸器系に与える影響に関する知見は乏しい。本研究では、平成 20 年度に引き続き、健常な大学生を対象に肺機能検査を毎日繰り返して行ってもらい、対象者のアレルギー素因等を考慮した上で、大気中粒子状物質及びオゾンが呼吸器系に与える影響について検討した。

B．研究方法

東京都内に居住し、都内の大学に通学している女子大学生20名(18～23歳)に電子式ピークフローメータ(Vitalograph社製)を１台ずつ渡して、2008年7月、10月、2009年1月、4月、7月、10月、2010年1月の7回、それぞれ約2週間ずつ連続して毎日朝と夜の1日2回、最大呼気流量(PEF)と1秒量(FEV_1)の自己測定を行ってもらった。また、アレルギー素因の有無を評価するために調査開始時に採血を行い、血清総IgE値、ダニ特異IgEを測定した。

大気汚染濃度は、対象者居住地の近傍にある大気環境測定局で測定されている浮遊粒子状物質(SPM)、二酸化窒素(NO_2)、オゾンを主成分とする光化学オキシダント(Ox)濃度を用いた。また、同測定局における気温、湿度も解析に用いた。

解析は一般化推定方程式 (GEE) により、対象者の身長、アレルギー素因の有無、気温、湿度の影響を調整し、大気汚染物質濃度が増加した時のPEF及びFEV_1値の変化量を評価した。

（倫理面への配慮）

兵庫医科大学倫理委員会の承認を得て、対象者から文書による同意を得た。

C．研究結果

対象者のうち、血清総IgE値が170 IU/ml以上またはダニ特異IgE抗体陽性でアレルギー素因を有すると考えられた者は12名、アレルギー素因がないと考えられた者は8名であった。各検査時期に朝は平均226.0回、夜は平均221.4回、合計ではそれぞれのべ1,582回、1,550回の測定結果が得られた。

朝のPEF値は、2009年7月は大気中SPM及びNO_2、2009年10月はOxの24時間平均濃度（前日午前6時～当日午前6時）が増加すると有意に低下するという関連性が認められた。同様に、夜のPEF値は、2010年1月のSPMの24時間平均濃度（前日午前6時～当日午前6時）が増加すると有意に低下するという関連がみられた。

朝のFEV_1値は、2008年10月のSPM及びNO_2濃度、2009年10月のOx、2010年1月のSPM濃度、夜のFEV_1値は2009年10月のOx濃度と2010年1月のNO_2濃度が増加すると有意な低下が観察された。

全期を合わせた解析では、朝、夜の PEF 値、FEV_1 値ともに大気汚染物質濃度との間に有意な関連は認められなかった。アレルギー素因の有無別にみたところ、アレルギー素因を有する者では、NO_2 の 24 時間平均濃度が 10ppb 増加すると、朝の FEV_1 値が 24.7ml（95%信頼区間 4.1, 45.3）低下し、夜の PEF 値が 2.85L/min（95%信頼区間 0.49, 5.22）低下するという有意な負の関連が認められた。しかし、SPM 及び Ox 濃度との間に有意な関連は認められなかった。

D．考察

自動車排出ガス等による大気中粒子状物質が健康に与える影響が懸念されている。大気汚染物質濃度の変動が呼吸器系に与える短期的影響については、気管支喘息等の呼吸器疾患を有する患者を対象とした研究成果は数多く報告されているが、健常者についての知見は乏しい。

本研究では、健常な女子大学生を対象に、2年間にわたって各季節に約2週間ずつ、毎日朝と夜に繰り返し実施してもらい、その間の大気汚染物質濃度の変動との関連を検討した。PEF値及びFEV_1値は大気中粒子状物質濃度をはじめとする汚染物質濃度との間に有意な負の相関が認められる時期があり、アレルギー素因を有する者では全期を通した解析でも大気中NO_2濃度との関連が有意であった。しかし、SPM及びOx濃度と肺機能との関連は、検査時期や実施の時間帯により、必ずしも一貫性のある結果は得られなかった。

今回の対象は健常者であったため、大気汚染の肺機能への影響が認められにくかったものと思われる。しかし、肺機能には様々な因子が影響していると考えられることから、大気汚染物質以外の因子についてさらに検討する必要があろう。

E．結論

東京都内で生活している女子大学生を対象に、2年間にわたって各季節に約2週間ずつ、毎日朝と夜に繰り返し実施してもらい、その間の大気汚染物質濃度の変動との関連性を検討した。

PEF値及びFEV_1値は、大気中SPM、Ox、NO_2濃度の増加によって有意に低下するという関連性が認められる時期があったが、検査時期や実施の時間帯により、必ずしも一貫性のある結果は得られなかった。全期を通した解析では、アレルギー素因を有する者では大気中NO_2濃度との関連が有意であったが、SPM及びOx濃度と肺機能との関連は認められなかった。アレルギー素因のないものではこうした関連はまったく見られなかった。

以上より、健常者では大気汚染の肺機能への影響は認められにくいが、アレルギー素因を有する者では NO_2 の影響が示唆された。

G．研究発表

1． 論文発表

1. Yamazaki S, Shima M, Ando M, Nitta H. Modifying effect of age on the association between ambient ozone and nighttime primary care visits due to asthma attack. J Epidemiol 19: 143-151, 2009.
2. Shima M, Yoda Y. An ecological study of lung cancer mortality and severe air pollution in the 1960s in an industrial city in Japan. Asian Journal of Atmospheric Environment 3: 9-18, 2009
3. 島正之．微小粒子状物質の健康影響．日本医事新報 4442, 60-64, 2009

2． 学会発表

1. 島正之．大気汚染の健康影響の新たな課題：微小粒子とオゾン．（サテライトシンポジウム）第68回日本公衆衛生学会総会，奈良（2009年10月）日本公衆衛生雑誌, 56, 59 2009)
2. 余田佳子，田村憲治，櫻井四郎，島正之．大気汚染物質が女子大学生の肺機能に与える短期的影響．第50回大気環境学会年会，横浜（2009年9月）（第50回大気環境学会年会講演要旨集，341, 2009.）

H．知的財産権の出願・登録状況（予定を含む。）

1. 特許取得

なし

2. 実用新案登録

なし

3.その他

なし

厚生労働科学研究費補助金(地球規模保健課題推進研究事業（国際医学協力研究事業）)
分担研究報告書

ナノ粒子・ナノマテリアルの呼吸器、免疫への影響

研究分担者　　高野裕久　　独立行政法人　国立環境研究所　環境健康研究領域　領域長

研究要旨

Vehicle、3 種類の粒径（15nm、50nm、100nm）の二酸化チタン（TiO_2）、細菌由来リポ多糖（LPS)の単独、または、LPS と TiO_2の併用群を設定し、マウスに経気道曝露した。曝露後、肺炎症に及ぼす影響とそのメカニズムについて検討した。結果として、LPS と TiO_2の併用曝露は、マウスの肺炎症を増悪した。特に、LPS と 50nm 以下の TiO_2の併用群では、肺組織と血中のサイトカイン・ケモカインおよび凝固因子のレベルが、LPS 単独群より上昇していた。TiO_2のナノマテリアルは、感染症に関連する肺炎症を増悪すること、また、その影響は小さいサイズでより強いことが示唆された。

A．研究目的

本研究では、ナノマテリアルが感染症関連肺炎症に及ぼす影響を明らかにすることを目的とし、ナノメーターサイズの二酸化チタン（TiO_2）粒子と 細菌由来リポ多糖（LPS）の曝露が、マウスの肺炎症に及ぼす影響とそのメカニズムについて検討した。

B．研究方法

TiO_2は、3種類のサイズ(15nm、50nm、100nm)を使用し、曝露前に250℃、2時間加熱処理した。ICRマウス（♂、6週齢）は、8群に分け、vehicle、TiO_2（8 mg/kg)、LPS（2.5 mg/kg）を単独、または、LPSとTiO_2を併用して経気道曝露した。曝露から24時間後に、肺胞洗浄液中の細胞構成、肺の血管透過性、肺または血中の炎症性サイトカイン・ケモカイン（interleukin (IL)-1βや macrophage chemoattractant protein (MCP)-1、 and keratinocyte chemoattractant (KC)）、血中の凝固関連因子（fibrinogenおよび von Willebrand factor (vWF) とprotein C (PC) 活性）について解析した。

（倫理面への配慮）

全ての動物実験は、動物愛護に配慮し、当該施設の担当委員会の承認の基に遂行した。

C．研究結果

LPSおよびTiO_2の単独曝露は、vehicleに比べて、肺胞洗浄液中の総細胞数と好中球数、タンパク量、肺水分量を増加あるいは増加する傾向が観察された（表1）。これらの肺炎症と血管透過性の亢進は、LPS 単

独曝露に比べて、LPSと50nm以下のTiO_2の併用曝露でより顕著に観察された。

LPSおよびTiO_2の単独曝露は、肺組織中におけるIL-1β等のサイトカインやMCP -1、KC等のケモカインの発現も誘導した（図1）。また、LPSとTiO_2の併用曝露では、LPS単独曝露に比べて、肺組織中および血中の炎症性サイトカイン・ケモカインが増加することや（図1、2）、凝固因子であるfibrinogenと内皮細胞傷害の指標であるvWFの血中レベルが増加すること、凝固制御因子であるPC活性が低下することを明らかにした（表2）。さらに、100nmのTiO_2よりも、15nmと50nmのTiO_2の方が、活性が強かった。

D．考察

本研究は、TiO_2の経気道曝露が、LPSによって誘導される肺における好中球性炎症と血管透過性亢進をさらに増悪することを明らかにした。その増悪には、肺局所での炎症性サイトカイン・ケモカインの増加が寄与していることが示唆された。また、LPSとTiO_2の併用曝露は、LPS単独曝露に比べて、血中の凝固因子の増加と凝固制御因子の低下を誘導すること、炎症性サイトカイン・ケモカインのレベルを増加することも示した。さらに、これらの増悪影響は、概して粒子のサイズがより小さいほどより強くなる傾向が観察された。

我々は、ラテックスやカーボンナノ粒子を用いた実験においても、本研究と同様の結果を見出している。また、これまでの報告から、サイズの小さいものほど、肺の深部に侵入し、循環器系に影響を及ぼす可能性があることも示唆されている。

以上のことから、環境中に存在するナノマテリアルの曝露は、炎症性因子の増加や凝固系障害を介して、LPSに誘導される肺の炎症と血管透過性をさらに亢進し、呼吸器・循環器系疾患を増悪する可能性がある。

E．結論

本研究は、日米、アジアでもリスクが危惧されているナノマテリアルと感染症関連疾患の関係について検討を行い、ナノマテリアルが感染症に関連する肺炎症を増悪すること、さらにその増悪影響のリスクは、サイズが小さいほど高いことを明らかにした。

環境中に存在するナノメーターサイズの粒子や工業的に生産されるナノマテリアルの経気道曝露は、循環器・呼吸器系疾患を持つ高感受性集団に対して、増悪影響を及ぼす可能性が示唆された。今後、更なる詳細なナノマテリアルの健康影響評価が必要である。

G．研究発表

1．論文発表

1. Inoue K, Takano H, Yanagisawa R, Koike E, Shimada A. Size effects of latex nanomaterials on lung inflammation in mice. Toxicol Appl Pharmacol, 234: 68-76, 2009.
2. Inoue K, Koike E, Yanagisawa R, Hirano S, Nishikawa M, Takano H. Effects of multi-walled carbon nanotubes on a murine allergic airway inflammation model. Toxicol Appl Pharmacol, 237: 306-316, 2009.
3. Yanagisawa R, Takano H, Inoue K, Koike

E, Kamachi T, Sadakane K, Ichinose T: Titanium dioxide nanoparticles aggravates atopic dermatitis-like skin lesions in NC/Nga mice. Exp Biol Med, 234: 314-322, 2009.

2. 学会発表

1. 井上健一郎、柳澤利枝、小池英子、高野裕久、工業用ナノマテリアルが呼吸器の脆弱状態へ及ぼす修飾影響、第49回日本呼吸器学会学術講演会、2009年
2. Inoue K, Takano H, Yanagisawa R, Koike E, Shimada A. Impacts of latex nanomaterials on sensitive lung inflammation. HORIBA International Conference CDBIM Symposium, 2009.

H. 知的財産権の出願・登録状況

1. 特許取得

なし

2. 実用新案登録

なし

3. その他

なし

表1. TiO_2およびLPSの経気道曝露が肺胞洗浄液中の総細胞数と好中球数、タンパク濃度、および肺水分量に及ぼす影響

Treatment	Total cells	Neutrophils	Protein	Lung wet weight - dry weight [mg]/body weight [g]
	($\times 10^4$/total BAL fluid)		(mg/ml of BAL fluid)	
vehicle	70.3 ± 7.1	21.4 ± 2.9	0.32 ± 0.02	4.17 ± 0.11
15 nm TiO_2	75.9 ± 24.6	37.5 ± 3.9	0.47 ± 0.04	4.74 ± 0.05 *
50 nm TiO_2	81.6 ± 36.6	44.6 ± 7.4 *	0.50 ± 0.03	4.63 ± 0.12 *
100 nm TiO_2	127.8 ± 34.9	81.1 ± 9.7 *	0.45 ± 0.03	4.52 ± 0.08
LPS	584.4 ± 47.3 **	511.7 ± 42.2 **	0.59 ± 0.06 *	6.72 ± 0.11 **
LPS + 15 nm TiO_2	725.0 ± 116.0 **#$	647.6 ± 105.6 **#$	0.95 ± 0.07 **#$	7.69 ± 0.20 **##$
LPS + 50 nm TiO_2	711.6 ± 155.4 **$	621.1 ± 136.8 **$	1.14 ± 0.15 **##$	7.43 ± 0.21 **##$
LPS + 100 nm TiO_2	547.2 ± 46.5 **$	476.3 ± 43.1 **$	1.08 ± 0.09 **##$	7.67 ± 0.20 **##$

気管内投与 24 時間後にマウスの肺胞洗浄液を採取し、肺胞洗浄液中の総細胞と好中球の数およびタンパク濃度を測定した。また、別の実験において肺を採取し、肺水分量を測定した。結果は平均値 ± SE で示した (n=8)。

* $P < 0.05$ versus the vehicle group, ** $P < 0.01$ versus the vehicle group, # $P < 0.05$ versus the LPS group, ## $P < 0.01$ versus the LPS group, $ $P < 0.01$ versus the nanomaterial group

表2. TiO_2およびLPSの経気道曝露が血中の凝固関連因子のレベルに及ぼす影響

Treatment	Fibrinogen	vWF	Activity of PC
	(mg/dl)	(%)	
vehicle	359.0 ± 7.1	73.4 ± 5.9	4.6 ± 0.7
15 nm TiO_2	405.5 ± 17.1	71.9 ± 5.2	4.9 ± 0.4
50 nm TiO_2	424.0 ± 18.1	66.4 ± 7.0	4.9 ± 0.2
100 nm TiO_2	439.0 ± 17.7 *	64.9 ± 4.1	4.9 ± 0.2
LPS	654.8 ± 24.1 **	90.4 ± 7.2 **	3.5 ± 0.2 *
LPS + 15 nm TiO_2	833.0 ± 25.2 **##$	104.4 ± 3.0 **##$	2.4 ± 0.2 **$
LPS + 50 nm TiO_2	765.5 ± 42.6 **#$	105.0 ± 5.3 **##$	2.8 ± 0.3 **$
LPS + 100 nm TiO_2	745.4 ± 27.5 **#$	99.9 ± 8.0 **#$	2.7 ± 0.3 **$

気管内投与 24 時間後にマウスの血液を採取し、血漿中の fibrinogen と vWF、PC 活性を測定した。結果は平均 ± SE で示した (n=8-10)。

* $P < 0.05$ versus the vehicle group, ** $P < 0.01$ versus the vehicle group, # $P < 0.05$ versus the LPS group, ## $P < 0.01$ versus the LPS group, $ $P < 0.01$ versus the nanomaterial group

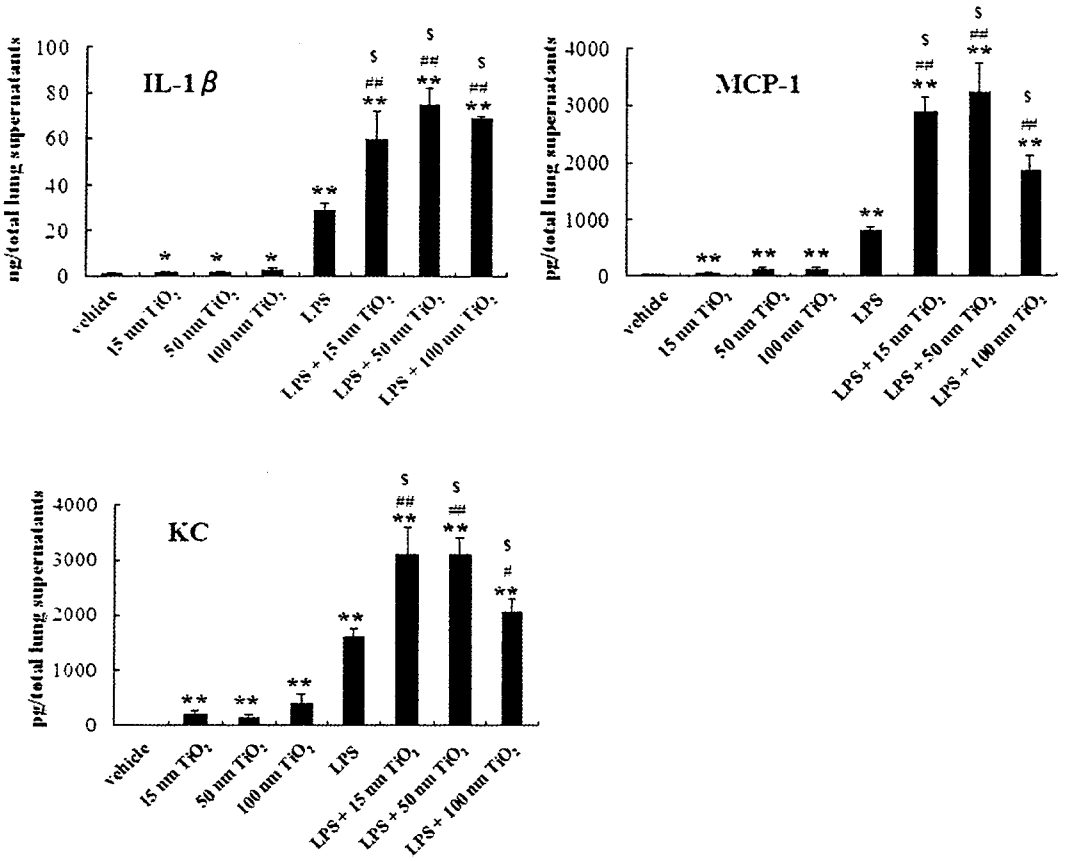

図 1.　TiO_2 および LPS の経気道曝露が肺組織中のサイトカイン・ケモカインのタンパクレベルに及ぼす影響

気管内投与 24 時間後にマウスの肺を採取し、肺組織懸濁液上清中の IL-1β と MCP-1、KC の含有量を測定した。結果は平均値 ± SE で示した (n=8)。
* P < 0.05 versus the vehicle group, ** P < 0.01 versus the vehicle group, # P < 0.05 versus the LPS group, ## P < 0.01 versus the LPS group, $ P < 0.01 versus the nanomaterial group.

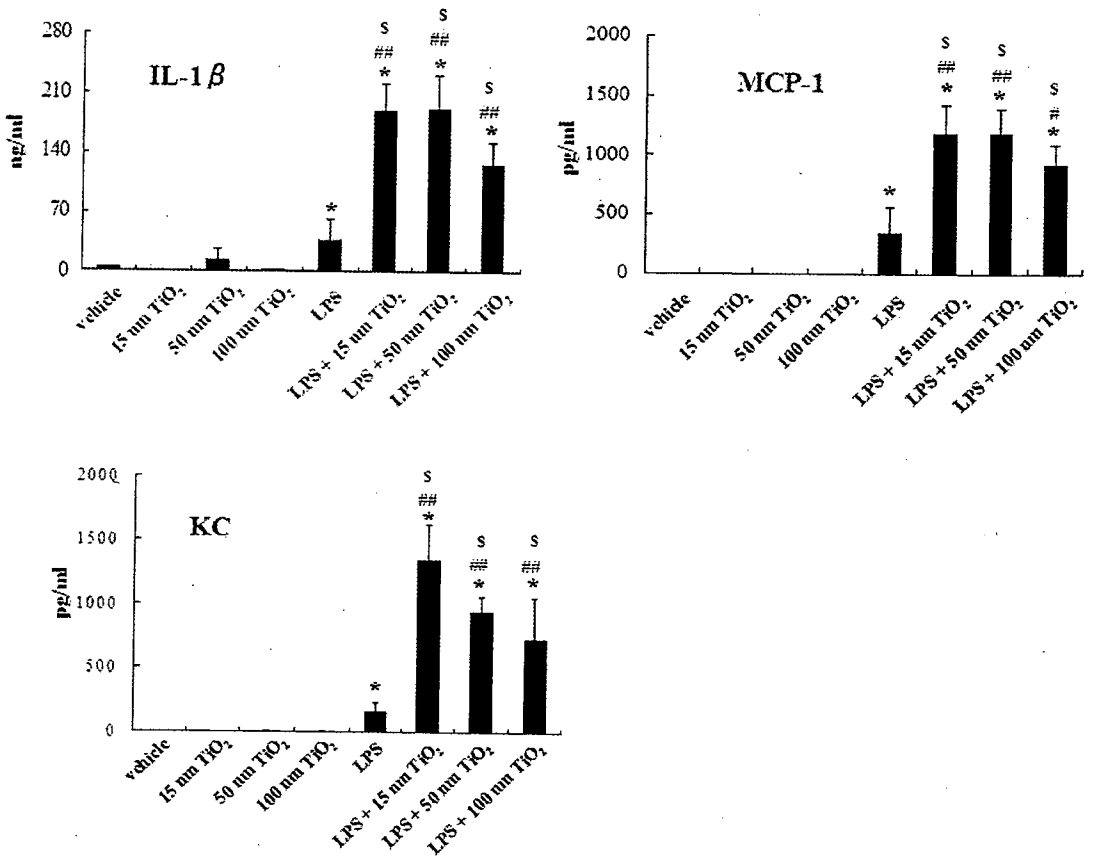

図 2. TiO_2 および LPS の経気道曝露が血中のサイトカイン・ケモカインのレベルに及ぼす影響

気管内投与 24 時間後にマウスの血液を採取し、血中の IL-1β と MCP-1、KC のレベルを測定した。結果は平均値 ± SE で示した (n=10)。

* P < 0.01 versus the vehicle group, # P < 0.05 versus the LPS group, ## P < 0.01 versus the LPS group, $ P < 0.01 versus the nanomaterial group.

別紙４

研究成果の刊行に関する一覧表

書籍

著者氏名	論文タイトル名	書籍全体の編集者名	書　籍　名	出版社名	出版地	出版年	ページ

雑誌

発表者氏名	論文タイトル名	発表誌名	巻号	ページ	出版年
Fukuda H, Takamura-Enya T, Masuda Y, Nohmi T, Seki C, Kamiya K, Sugimura T, Masutani C, Hanaoka F, Nakagama H	Translesional DNA synthesis through a C8-guanyl adduct of 2-amino-1-methyl-6-phenylimidazo[4,5-*b*]pyridine (PhIP) in Vitro: REV1 inserts dC opposite the lesion, and DNA polymerase kappa potentially catalyzes extension reaction from the 3'-dC terminus	J Biol Chem	284	25585-25592	2009
Okamoto K, Taya Y, Nakagama H	Mdmx enhances p53 ubiquitination by altering the substrate preference of the Mdm2 ubiquitin ligase	FEBS Lett	583	2710-2714	2009
Endo H, Hosono K, Fujisawa T, Takahashi H, Sugiyama M, Yoneda K, Nozaki Y, Fujita K, Yoneda M, Inamori M, Wada K, Nakagama H, Nakajima A	Involvement of JNK pathway in the promotion of the early stage of colorectal carcinogenesis under high-fat dietary conditions	Gut	58	1637-1643	2009
Ohtsubo C, Shiokawa D, Kodama M, Gaiddon C, Nakagama H, Jochemsen AG, Taya Y, Okamoto K	Cytoplasmic tethering is involved in synergistic inhibition of p53 by Mdmx and Mdm2	Cancer Sci	100	1291-1299	2009

発表者氏名	論文タイトル名	発表誌名	巻号	ページ	出版年
Sugiyama M, Takahashi H, Hosono K, Endo H, Kato S, Yoneda K, Nozaki Y, Fujita K, Yoneda M, Wada K, Nakagama H, Nakajima A	Adiponectin inhibits colorectal cancer cell growth through the AMPK/mTOR pathway	Int J Oncol	34	339-344	2009
Takahashi H, Takayama T, Yoneda K, Endo H, Iida H, Sugiyama M, Fujita K, Yoneda M, Inamori M, Abe Y, Saito S, Wada K, Nakagama H, Nakajima A	Association of visceral fat accumulation and plasma adiponectin with rectal dysplastic aberrant crypt foci in a clinical population	Cancer Sci	100	29-32	2009
Kawanishi M, Nishida H, Totsuka Y, Nishimura K, Wakabayashi K, Yagi T	Mutagenic specificity of *N*-nitrosotaurocholic acid in *supF* shuttle vector plasmids.	Genes Environ.	31	9-14	2009
Matsuda Y, Takeuchi H, Yokohira M, Saoo K, Hosokawa K, Yamakawa K, Zeng Y, Totsuka Y, Wakabayashi K, Imaida K.	Enhancing effects of a high fat diet on 2-amino-3,8-dimethylimidazo[4,5-*f*]quinoxaline-induced lung tumorigenesis in female A/J mice	Mol. Med. Rep.,	2.	701-706	2009
Ohe T, Suzuki A, Watanabe T, Hasei T, Nukaya H, Totsuka Y, Wakabayashi K	. Induction of SCEs in CHL cells by dichlorobiphenyl-derivative water pollutants, 2-phenylbenzotriazole (PBTA) congeners and river water concentrates.	Mutat. Res.,	678	38-42	2009
Ozeki M, Muroyama A, Kajimoto T, Watanabe T, Wakabayashi K, Node M	Synthesis of a new mutagenic benzoazepinoquinolinone derivative.	Synlett,	11	1781-1784	2009
Yamamoto M, Nakano T, Matsushima-Hibiya Y, Totsuka Y, Takahashi-Nakaguchi A, Matsumoto Y, Sugimura T, Wakabayashi K	Molecular cloning of apoptosis-inducing Pierisin-like proteins, from two species of white butterfly, *Pieris melete* and *Aporia crataegi*.	Comp. Biochem. Physiol. B Biochem. Mol. Biol.,	154	326-333	2009

発表者氏名	論文タイトル名	発表誌名	巻号	ページ	出版年
Totsuka Y, Higuchi T, Imai T, Nishikawa A, Nohmi T, Kato T, Masuda S, Kinae N, Hiyoshi K, Ogo S, Kawanishi M, Yagi T, Ichinose T, Fukumori N, Watanabe M, Sugimura T, Wakabayashi K	Genotoxicity of nano/microparticles in *in vitro* micronuclei, *in vivo* comet and mutation assay systems.	Part. Fibre. Toxicol.,	6	23	2009
Nishigaki R, Watanabe T, Kajimoto T, Tada A, Takamura-Enya T, Enomoto S, Nukaya H, Terao Y, Muroyama A, Ozeki M, Node M, Hasei T, Totsuka Y, Wakabayashi K	Isolation and identification of a novel aromatic amine mutagen produced by the Maillard reaction.	Chem. Res. Toxicol.,	22	1588-1593	2009
Nishimura K, Totsuka Y, Higuchi T, Kawahara N, Sugimura T, Wakabayashi K	Analysis of an RNA adduct formed from aminophenylnorharman.	Nucleic Acids Symp. Ser. (Oxf.),	53	211-212	2009
Mutoh M, Komiya M, Teraoka N, Ueno T, Takahashi M, Kitahashi T, Sugimura T, Wakabayashi K	Overexpression of low-density lipoprotein receptor and lipid accumulation in intestinal polyps in Min mice.	Int. J. Cancer,	125	2505-2510	2009
Yamaji T, Iwasaki M, Sasazuki S, Kurahashi N, Mutoh M, Yamamoto S, Suzuki M, Moriyama N, Wakabayashi K, Tsugane S	Visceral fat volume and the prevalence of colorectal adenoma.	Am. J. Epidmiol.,	170	1502-1511	2009
Wakabayashi, K.	Chemical and biological approaches for detecting environmental causes of cancer.	Genes Environ.,	31	87-96	2009
Murakami Y, Imai N, Miura T, Sugimura T, Wakabayashi K, Totsuka Y, Hada N, Yokoyama Y, Suzuki H, Mitsunaga K	Chemical confirmation of the structure of a mutagenic aminophenylnorharman, 9-(4'-aminophenyl)-9*H*-pyrido[3,4-*b*]indole: An authentic synthesis of 9-(4'-nitrophenyl)-9*H*-pyrido[3,4-*b*]indole as its relay compound.	Heterocycles,	80	455-462,	2010

発表者氏名	論文タイトル名	発表誌名	巻号	ページ	出版年
Watanabe T, Tanaka G, Hamada S, Namiki C, Suzuki T, Nakajima M, Furihata C.	Dose-dependent alterations in gene expression in mouse liver induced by diethylnitrosamine and ethylnitrosourea and determined by quantitative real-time PCR.	Mutat Res.	673	9-20	2009
Yamaguchi T, Suzuki T, Arai H, Tanabe S, Atomi Y.	Continuous mild heat stress induces differentiation of mammalianmyoblasts, shifting fiber type from fast to slow.	Am. J. Physiol. Cell Physiol.	298	140-148	2010
Hasei T, Watanabe T, Endo O, Sugita K, Asanoma M, Goto S, Hirayama T	Determination of 3,6-dinitrobenzo[*e*]pyrene in surface soil and airborne particles, and its possible sources, diesel particles and incinerator dusts	Journal of Health Science	55	567-577	2009
Kawanishi M, Watanabe T, Hagio S, Ogo S, Shimohara C, Jouchi R, Takayama S, Hasei T, Hirayama T, Oda Y, Yagi T	Genotoxicity of 3,6-dinitrobenzo[*e*]pyrene, a novel mutagen in ambient air and surface soil, in mammalian cells *in vitro* and *in vivo*	Mutagenesis	24	279-284	2009
Oda Y, Hirayama T, Watanabe T	Genotoxic activation of the environmental pollutant 3,6-dinitrobenzo[*e*]pyrene in *Salmonella typhimurium* umu strains expressing human cytochrome P450 and *N*-acetyltransferase	Toxicology Letters	188	258-262	2009
Yamazaki, S., Shima, M., Ando, M., Nitta, H.	Modifying effect of age on the association between ambient ozone and nighttime primary care visits due to asthma attack.	J. Epidemiol.	19	143-151	2009
Shima, M., Yoda, Y.	An ecological study of lung cancer mortality and severe air pollution in the 1960s in an industrial city in Japan.	Asian Journal of Atmospheric Environment	3	9-18	2009
島正之	微小粒子状物質の健康影響.	日本医事新報	4442	60-64	2009
Inoue K, Takano H, Yanagisawa R, Koike E, Shimada A	Size effects of latex nanomaterials on lung inflammation in mice.	Toxicol Appl Pharmacol	234	68-76	2009
Inoue K, Koike E, Yanagisawa R, Hirano S, Nishikawa M, Takano H	Effects of multi-walled carbon nanotubes on a murine allergic airway inflammation model.	Toxicol Appl Pharmacol	237	306-316	2009
Yanagisawa R, Takano H, Inoue K, Koike E, Kamachi T, Sadakane K, Ichinose T	Titanium dioxide nanoparticles aggravates atopic dermatitis-like skin lesions in NC/Nga mice.	Exp Biol Med	234	314-322	2009

THE JOURNAL OF BIOLOGICAL CHEMISTRY VOL. 284, NO. 38, pp. 25585–25592, September 18, 2009

Translesional DNA Synthesis through a C8-Guanyl Adduct of 2-Amino-1-methyl-6-phenylimidazo[4,5-*b*]pyridine (PhIP) *in Vitro*

REV1 INSERTS dC OPPOSITE THE LESION, AND DNA POLYMERASE κ POTENTIALLY CATALYZES EXTENSION REACTION FROM THE 3′-dC TERMINUS[*][S]

Received for publication, June 25, 2009, and in revised form, July 16, 2009 Published, JBC Papers in Press, July 23, 2009, DOI 10.1074/jbc.M109.037259

Hirokazu Fukuda[‡], Takeji Takamura-Enya[§], Yuji Masuda[¶], Takehiko Nohmi[‖], Chiho Seki[‡], Kenji Kamiya[¶], Takashi Sugimura[‡], Chikahide Masutani[**], Fumio Hanaoka[1], and Hitoshi Nakagama[‡2]**

From the [‡]Biochemistry Division, National Cancer Center Research Institute, 1-1, Tsukiji 5, Chuo-ku, Tokyo 104-0045, the [§]Department of Applied Chemistry, Faculty of Engineering, Kanagawa Institute of Technology, Ogino 1030, Atsugi, Kanagawa 243-0292, the [¶]Department of Experimental Oncology, Research Institute for Radiation Biology and Medicine, Hiroshima University, Kasumi 1-2-3, Minami-ku, Hiroshima, Hiroshima 734-8553, the [‖]Division of Genetics and Mutagenesis, National Institute of Health Sciences, Kamiyoga 1-18-1, Setagaya-ku, Tokyo 158-8501, and the [**]Cellular Biology Laboratory, Graduate School of Frontier Biosciences, Osaka University, Yamada-oka 1-3, Suita, Osaka 565-0871, Japan

2-Amino-1-methyl-6-phenylimidazo[4,5-*b*]pyridine (PhIP) is the most abundant heterocyclic amine in cooked foods, and is both mutagenic and carcinogenic. It has been suspected that the carcinogenicity of PhIP is derived from its ability to form DNA adducts, principally dG-C8-PhIP. To shed further light on the molecular mechanisms underlying the induction of mutations by PhIP, *in vitro* DNA synthesis analyses were carried out using a dG-C8-PhIP-modified oligonucleotide template. In this template, the dG-C8-PhIP adduct was introduced into the second G of the TCC GGG AAC sequence located in the 5′ region. This represents one of the mutation hot spots in the rat *Apc* gene that is targeted by PhIP. Guanine deletions at this site in the *Apc* gene have been found to be preferentially induced by PhIP in rat colon tumors. DNA synthesis with A- or B-family DNA polymerases, such as *Escherichia coli* polymerase (pol) I and human pol δ, was completely blocked at the adducted guanine base. Translesional synthesis polymerases of the Y-family, pol η, pol ι, pol κ, and REV1, were also used for *in vitro* DNA synthesis analyses with the same templates. REV1, pol η, and pol κ were able to insert dCTP opposite dG-C8-PhIP, although the efficiencies for pol η and pol κ were low. pol κ was also able to catalyze the extension reaction from the dC opposite dG-C8-PhIP, during which it often skipped over one dG of the triple dG sequence on the template. This slippage probably leads to the single dG base deletion in colon tumors.

Heterocyclic amines (HCAs)[3] are naturally occurring genotoxic carcinogens produced from cooking meat (1). The initial carcinogenic event induced by HCAs is metabolic activation and subsequent covalent bond formation with DNA (1, 2). 2-Amino-1-methyl-6-phenylimidazo[4,5-*b*]pyridine (PhIP) is the most abundant heterocyclic amine in cooked foods, and was isolated from fried ground beef (3, 4). PhIP possesses both mutagenic and carcinogenic properties (5–8). Epidemiological studies have revealed that a positive correlation exists between PhIP exposure and mammary cancer incidence (9). PhIP induces colon and prostate cancers in male rats and breast cancer in female rats (8, 10).

The incidences of colon, prostate, and breast cancers are steadily increasing in Japan and other countries and this has been found to correlate with a more Westernized lifestyle. Elucidating the molecular mechanisms underlying PhIP-induced mutations is therefore of considerable interest. It is suspected that the carcinogenicity of PhIP is derived from the formation of DNA adducts, principally dG-C8-PhIP (11–14) (see Fig. 1). Studies of the mutation spectrum of PhIP in mammalian cultured cells and transgenic animals have revealed that G to T transversions are predominant and that guanine deletions from G stretches, especially from the 5′-GGGA-3′ sequence, are significant (15–20). Five mutations in the *Apc* gene were detected in four of eight PhIP-induced rat colon tumors, and all of these mutations involved a single base deletion of guanine from 5′-GGGA-3′ (21). These mutation spectra are thought to be influenced by various factors, including the primary structure of the target gene itself, the capacity of translesional DNA polymerases, and the activity level of repair enzymes (1). However, the molecular mechanisms underlying the formation of PhIP-induced mutations are largely unknown.

To shed further light on the molecular processes that underpin the mutations induced by PhIP, we performed *in vitro* DNA synthesis analyses using a dG-C8-PhIP-modified oligonucleotide template. We have recently reported the successful synthesis of oligonucleotides harboring a site-specific PhIP adduct

* This work was supported by Kakenhi Grant 19570144.
[S] The on-line version of this article (available at http://www.jbc.org) contains supplemental Table S1 and Figs. S1–S6.
[1] Present address: Dept. of Life Science, Faculty of Science, Gakushuin University, Mejiro 1-5-1, Toshima-ku, Tokyo 171-8588, Japan.
[2] To whom correspondence should be addressed. Tel.: 81-3-3542-2511; Fax: 81-33542-2530; E-mail: hnakagam@ncc.go.jp.
[3] The abbreviations used are: HCA, heterocyclic amines; PhIP, 2-amino-1-methyl-6-phenylimidazo[4,5-*b*]pyridine; TLS, translesional DNA synthesis; IQ, 2-amino-3-methylimidazo[4,5-*f*]quinoline; pol, DNA polymerase; DTT, dithiothreitol; PCNA, proliferating cell nuclear antigen; PIPES, 1,4-piperazinediethanesulfonic acid.

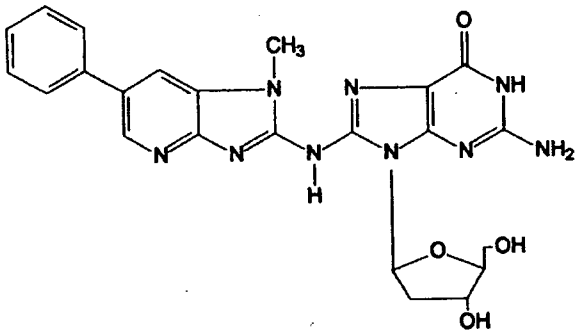

dG-C8-PhIP

FIGURE 1. **Structure of the dG-C8-PhIP adduct.**

(22). In our current study, we used this synthesis method to construct a 32-mer oligonucleotide template containing a 5′-TTCGGGAAC-3′ sequence with different site-specific PhIP adducts. We then utilized the resulting constructs in DNA synthesis analyses to reconstitute the PhIP-induced mutagenesis of the rat *APC* gene. DNA synthesis reactions with A- or B-family DNA polymerases, such as *Escherichia coli* pol I and human pol δ, or translesional synthesis (TLS) polymerases of the Y-family, pol η, pol ι, pol κ, and REV1, were carried out. Kinetic analyses of pol κ and REV1, for which TLS activities at the PhIP adduct were detected, were also performed.

EXPERIMENTAL PROCEDURES

Enzymes and Materials—T4 polynucleotide kinase and T4 DNA ligase were purchased from Toyobo Biochem (Osaka, Japan) and Takara Biotech (Tokyo Japan), respectively. Other materials were obtained from Sigma or Wako (Osaka, Japan).

DNA Polymerases and PCNA—Human recombinant DNA polymerases, pol δ, pol η, pol κ, and REV1, and PCNA were expressed and purified as described previously (23–27). Human DNA polymerase α and DNA polymerase ι were purchased from Chimerx. *E. coli* DNA polymerases I (Takara Biotech) and Klenow Fragment (Takara Biotech), and thermophilic bacterial DNA polymerases, r*Taq* (Toyobo Biochem) and *Tth* (Toyobo Biochem) were used.

Oligonucleotides—The method used to chemically synthesize three 9-mer oligonucleotides, 5′-TCCGGGAAC-3′, containing a PhIP adduct on either the first, second, or third G (p9B, p9C, and p9D, respectively) has been described previously (22). All other synthetic oligonucleotides were synthesized and purified using a reverse-phase cartridge (Operon Biotech Japan (Tokyo, Japan). The 23-mer oligonucleotides: p23a, 5′-TGACTCGTCGTGACTGGGAAAAC-3′, and p23b, 5′-GTCACGACGAGTCAGTTCCCGGA-3′, were used for constructing the template oligonucleotides as described below. A 32-mer oligonucleotide without the PhIP adduct, p32A, was used as a control template (see Table 1). Its 3′ complementary 29-, 28-, 27-, 26-, 22-, and 17-mer sequences (p29, p28, p27, p26, p22, and p17) were used as extension primers (see Table 1).

Construction of Template-Primer Complexes Containing the PhIP Adduct—A 32-mer template oligonucleotide p32C (see Table 1) was constructed by ligation of p9C with p23a as follows. The 5′-end of p23a was phosphorylated by T4 polynucleotide kinase and ATP. A mixture of p9C, p23a, and p23b (3 nmol each) in 250 μl of a buffer containing 5 mM Tris-HCl, 0.5 mM EDTA, 50 mM NaCl, pH 8.0, was denatured for 5 min at 95 °C, incubated for 10 min at 60 °C, and then cooled slowly to form the partial duplex structure of these three oligonucleotides (supplemental Fig. S1). The sample of the duplex oligonucleotide was mixed with 190 μl of Milli-Q water and 50 μl of ×10 ligation buffer (500 mM Tris-HCl (pH 7.5), 100 mM $MgCl_2$, 100 mM DTT, 10 mM ATP). Ligation was initiated by adding 10 μl of T4 DNA ligase (4,000 units), and the mixture was then incubated for 20 h at 16 °C. An additional incubation at 37 °C for 60 min was carried out after the addition of 1 μl of T4 DNA ligase, and the reaction was stopped by further incubation at 68 °C for 10 min. The p32C was separated by 18% PAGE containing 8 M urea, and excised and eluted as described previously (28). p32B and p32D were constructed using a similar method as for p9B and p9D, respectively (see Table 1). The purities of these oligonucleotides, p32B, p32C, and p32D, were determined by denatured PAGE after 5′-end labeling and UV absorbance at 260 and 370 nm.

Primer oligonucleotides were labeled with ^{32}P at the 5′-end as described previously (29), and then purified by MicroSpin™ G-25 or G-50 columns (GE Healthcare) as recommended by the supplier. The mixture of template and labeled primer (50 pmol each) in 400 μl of a buffer containing 8 mM Tris-HCl, 0.8 mM EDTA, 150 mM KCl (pH 8.0) was heated at 70 °C for 7 min, and then cooled slowly to room temperature. In the case of the substrates for TLS polymerases, pol η, pol ι, pol κ, and REV1, the final concentrations of template-primer and the constituents of the annealing buffers were changed to 500 nM and 10 mM Tris-HCl, 1 mM EDTA, and 50 mM NaCl (pH 8.0), respectively.

In Vitro DNA Synthesis Assay—A primer extension reaction was performed as described previously (30) with some modifications. Briefly, an aliquot of 0.75 μl of this primer-annealed template (final concentration, 12.5 nM) was mixed with 0.75 μl of ×10 Klenow buffer (100 mM Tris-HCl (pH 7.5), 70 mM $MgCl_2$, 1 mM DTT), 0.5 μl of 500 mM KCl, 0.5 μl of dNTP mixture (50 μM each), and 4.5 μl of Milli-Q water. After addition of 0.5 μl of Klenow fragment, the mixture was incubated at 37 °C for 10 min. The reaction was terminated by adding 1.5 μl of stop solution (160 mM EDTA, 0.7% SDS, 6 mg/ml proteinase K), and the samples were incubated at 37 °C for 30 min. Subsequently, 5.5 μl of the gel loading solution (30 mM EDTA, 0.05% bromophenol blue, 0.05% xylene cyanol, 97% formamide) was added to the samples. For pol δ, a ×10 reaction buffer containing 200 mM PIPES (pH 6.8), 20 mM $MgCl_2$, 10 mM 2-mercaptethanol, 200 μg/ml bovine serum albumin, and 50% glycerol was used instead of the buffer described above, and the reaction was carried out at 37 °C for 10 min. For other DNA polymerases, pol α, pol I, r*Taq*, and *Tth*, the constituent of each ×10 reaction buffer was altered as recommended by the suppliers.

The reaction using pol κ was performed as described above with some modifications. Briefly, an aliquot of 0.5 μl of this primer-annealed template (final 50 nM) was mixed with 0.5 μl of 10 × TLS buffer (250 mM Tris-HCl (pH 7.0), 50 mM $MgCl_2$, 50 mM DTT, 1 mg/ml bovine serum albumin), 0.5 μl of dNTP solution, and 3.0 μl of Milli-Q water. After addition of 0.5 μl of pol κ, the mixture was incubated at 30 °C for 20 min. The reac-

tion was terminated by adding 8.8 μl of the gel loading solution and a further incubation at 95 °C for 3 min. The reaction of REV1 was performed in the same manner as the reaction of pol κ with the exception that the standard reaction time was 5 min. For pol η, a ×10 reaction buffer containing 400 mM Tris-HCl (pH 8.0), 10 mM $MgCl_2$, 100 mM DTT, 1 mg/ml bovine serum albumin, and 450 mM KCl was used instead of the ×10 TLS buffer. The ^{32}P-labeled fragments were denatured and electrophoresed in a 9.5% polyacrylamide gel containing 8 M urea. The radioactivity of the fragments was determined using a Bio-Imaging Analyzer (BAS2500, Fuji Photo Film, Kanagawa, Japan). Kinetic parameters were determined by steady-state gel kinetic assays under similar conditions as described above. The incubation time for pol κ was changed to 10 min. K_m and k_{cat} were evaluated from the plot of the initial velocity *versus* the dCTP or dGTP concentration using a hyperbolic curve-fitting program in SigmaPlot 11 (Systat Software, Inc.). Data from two or three independent experiments were plotted together.

RESULTS

Construction of Template Oligonucleotides Containing a PhIP Adduct—We designed oligonucleotides containing a dG-C8-PhIP adduct at specific sites for use as templates in *in vitro* DNA synthesis analyses. For this purpose, we selected the 5′-TCCGGGAAC-3′ sequence as: 1) it corresponds to codon 868–870 of the rat *Apc* gene, one of three mutation hot spots (a single base deletion of G) in PhIP-induced colon tumors (21), and could thus be used as a model template that would reconstitute mutations of this gene; 2) two other mutation hot spots in the rat *Apc* gene and many mutated sites induced by PhIP in cultured cells and animal models contain 5′-GGGA-3′ as a core sequence (17–20). We thus speculated that the 5′-TCCGGGAAC-3′ sequence could be used as a model sequence for these GGGA to GGA mutations to some extent; and 3) some mutagenic compounds forming dG adducts, including PhIP, are expected to react preferentially with the 5′-G of a GG dinucleotide site when compared with a single G residue (31). We thus selected a sequence containing GGG as a template for our initial analysis.

We have recently synthesized three 9-mer oligonucleotides separately harboring a PhIP adduct on each G within the sequence 5′-TCC GGG AAC-3′ (22). Three 32-mer template oligonucleotides, p32B, p32C, and p32D, were constructed in our present study by ligation of these 9-mer oligonucleotides containing the dG-PhIP adduct with a 23-mer oligonucleotide, p23a, (Table 1 and supplemental Fig. S1). The purities of these oligonucleotides were tested after resolution by electrophoresis. In our present study, we principally describe the results of our *in vitro* DNA synthesis analysis using p32C as the template to avoid complexity.

In Vitro DNA Synthesis by A- and B-family DNA Polymerase—Many of the chemical compounds that can form DNA adducts *in vivo* and that show mutagenicity have been reported to impede the progress of DNA synthesis to different extents. The molecular size of PhIP is greater than most other mutagenic chemicals that form adducts. Hence, dG-PhIP was expected to block DNA synthesis to a considerable extent. To examine the effects of the dG-C8-PhIP adduct upon DNA synthesis, primer

TABLE 1
Oligonucleotide templates and primers

Oligonucleotide	Sequence[a]
p32A	5′-TCC GGG AAC TGACTCGTC GTGACTGGG AAAAC-3′
p32B	5′-TCC **G**GG AAC TGACTCGTC GTGACTGGG AAAAC-3′
p32C	5′-TCC G**G**G AAC TGACTCGTC GTGACTGGG AAAAC-3′
p32D	5′-TCC GG**G** AAC TGACTCGTC GTGACTGGG AAAAC-3′
p29	5′-GTT TTC CCA GTCACGACG AGTCAGTTC CC-3′
p28	5′-GTT TTC CCA GTCACGACG AGTCAGTTC C-3′
p27	5′-GTT TTC CCA GTCACGACG AGTCAGTTC-3′
p26	5′-GTT TTC CCA GTCACGACG AGTCAGTT-3′
p22	5′-GTT TTC CCA GTCACGACG AGTC-3′
p17	5′-GTT TTC CCA GTCACGAC-3′

[a] The bold G indicates the site of the PhIP-C8-dG adduct. Underlined sequences correspond to codon 868–870 at nucleotides 2602–2610 of the rat APC gene.

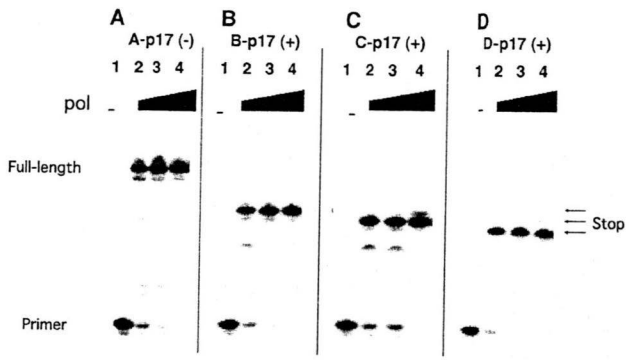

FIGURE 2. ***In vitro* DNA synthesis using Klenow fragment.** Gel electrophoresis indicating the primer extensions obtained using the 32-mer oligonucleotide templates, p32A (*A*), p32B (*B*), p32C (*C*), and p32D (*D*), which have no PhIP adduct, and a PhIP adduct on the first, second, and third G within the triple G sequence, respectively. The 3′ complementary 17-mer sequence, p17, was used as the extension primer. The final concentration of each template-primer complex was 12.5 nM. Concentrations of Klenow fragment were 0 (*lane 1*), 7.8 (*lane 2*), 23 (*lane 3*), and 78 units/ml (*lane 4*).

extension experiments using p32B, p32C, and p32D as templates were carried out (see Table 1). The length of each produced fragment was precisely determined using ladders of oligonucleotide fragments as markers (data not shown). The Klenow fragment of *E. coli* DNA polymerase I, a member of the A-family DNA polymerases, was first used in this analysis. The production of a 28-, 27-, and 26-mer from these primer extension reactions using B-p17, C-p17, and D-p17, respectively, using a template-primer complex, and lack of longer fragments indicated that the Klenow fragment stalled just before the dG-C8-PhIP adduct (Fig. 2). On the other hand, control experiments using p32A without the adduct as a template produced a 32-mer fragment (Fig. 2*A*). Similar results were obtained with *E. coli* DNA polymerase I (exo$^+$) and B-family DNA polymerases, such as the thermophilic bacterial DNA polymerases, r*Taq* and *Tth*, and human DNA polymerase α (data not shown) (supplemental Fig. S2), suggesting that stalling at the dG-C8-PhIP adduct occurs for all replicative DNA polymerases. Stalling of r*Taq* and *Tth* at the PhIP adduct was observed at 65 °C, as well as at 37 °C, indicating that this is the result of a physical hindrance of the adduct itself and not from secondary DNA structures. Moreover, there was no difference found between the stalling of *E. coli* DNA polymerase I (exo$^+$) and that of the Klenow fragment (exo$^-$). This indicates that the physical blocking of DNA polymerases at the dG-C8-PhIP adduct does not depend upon their proofreading function.

Finally, DNA synthesis analyses with human DNA polymerase δ (pol δ), a member of the B-family DNA polymerases and a truly replicative polymerase, were carried out. In the case of using p32C and p17 (C-p17) as a template-primer complex, the production of 27-mer fragments indicated the stalling of pol δ just before the PhIP adduct (Fig. 3, *lane 11*). From a control reaction using A-p17, a template-primer complex without the PhIP* adduct, a full-length product of 32-mer was generated (Fig. 3, *lane 8*). In addition to these major products, minor products extended one nucleotide further (28- and 33-mer) and ladders of bands indicating degradation of primer (<17-mer) were observed (Fig. 3), corresponding with previous results reporting terminal dA transferase and exonuclease activities of pol δ (32). PCNA, an accessory protein acting as a sliding clamp for pol δ, was previously reported to promote DNA synthesis by pol δ past several template lesions, including abasic sites, 8-oxo-dG, and aminofluorene-dG (32). In the case of dG-C8-PhIP, however, PCNA was unable to promote the bypass synthesis of pol δ beyond the lesion (Fig. 3, *lane 12*). Extension reaction from the longer 22-mer primer, p22, also paused completely just before the PhIP adduct in the presence or absence of PCNA (Fig. 3, *lanes 5* and *6*). These results strongly suggest that the dG-C8-PhIP adduct on genome DNA in the living cells induces the complete block of replication forks including pol δ, PCNA, and pol α.

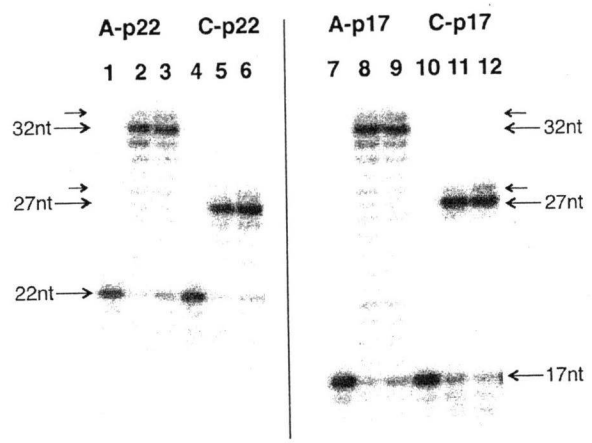

FIGURE 3. ***In vitro* DNA synthesis using pol δ in the presence or absence of PCNA.** Gel electrophoresis indicating the primer extensions obtained using the 32-mer oligonucleotide templates, p32A (*A*), and p32C (*C*), which have no PhIP adduct, and a PhIP adduct on the second G within the triple G sequence, respectively. The 3′ complementary 22- and 17-mer sequences, p22 and p17, were used as the extension primer. The final concentration of each template-primer complex was 12.5 nM. Concentrations of pol δ were 0 (*lanes 1, 4, 7,* and *10*) and 16 nM (*lanes 2, 3, 5, 6, 8, 9, 11,* and *12*). Concentrations of PCNA as a trimer were 0 (*lanes 1, 2, 4, 5, 7, 8, 10,* and *11*) and 20 nM (*lanes 3, 6, 9,* and *12*). *Large arrows* indicate the positions of primers (17- or 22-mer), full-length products (32-mer), and the products pausing just before the PhIP adduct (27-mer). *Small arrows* indicate the minor products that incorporated an additional 1 nucleotide (*nt*) to a full-length product or the pausing product.

Translesional DNA Synthesis by Y-family DNA Polymerases—Translesional DNA synthesis at the dG-C8-PhIP adduct by the Y-family DNA polymerases, pol η, pol κ, pol ι, and REV1 was next examined. Two substrates, C-p27 and C-p28, and their counterparts without a PhIP adduct, A-p27 and A-p28, were used in these experiments (Fig. 4). Substrate C-p27 was prepared by annealing the p32C template (see Table 1) to its 3′-complimentary 27-mer sequence, p27, and was used to identify the nucleotides that are inserted opposite the dG-C8-PhIP adduct (Fig. 4). Similarly, substrate C-p28 was used to analyze the extension reaction from the 3′-end of the dC bases opposite the dG-C8-PhIP adduct (Fig. 4). We found that recombinant human DNA polymerase η (pol η) could insert a dC opposite the dG-C8-PhIP adduct, although at low efficiency compared with control experiments without the PhIP adduct (Fig. 5, *A* and *B*). Extension reactions catalyzed by pol η from the 3′-end of dC opposite the adduct were barely detectable (Fig. 5*D*), although an excessive amount of pol η produced byproducts that incorporated a mismatch nucleotide, dG, dA, or dT (supplemental Fig. S4). In the case of dG, incorporation of one to three dG nucleotides was observed (supplemental Fig. S4). In control experiments without the PhIP adduct, minor products were produced that incorporated mismatch nucleotides, in addition to a major product that incorporated a dC (Fig. 5*C*).

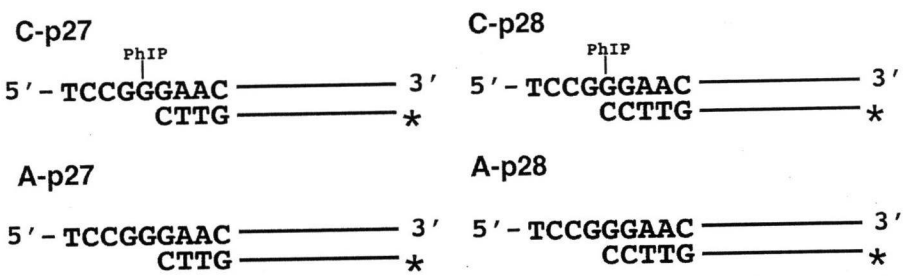

FIGURE 4. **Template-primer complexes.** Substrates C-p27 and C-p28 (series-C) have a PhIP adduct on the second dG within a GGG sequence. Substrates A-p27 and A-p28 (series-A) are control substrates without a PhIP adduct. The corresponding 3′ complimentary 27- and 28-mer sequences, p27 and p28, were used as extension primers. The template-primer complexes, C-p27 and C-p28, were used to monitor the nucleotide insertions into the site opposite dG-C8-PhIP and the extension reactions from the 3′-dC opposite dG-C8-PhIP, respectively.

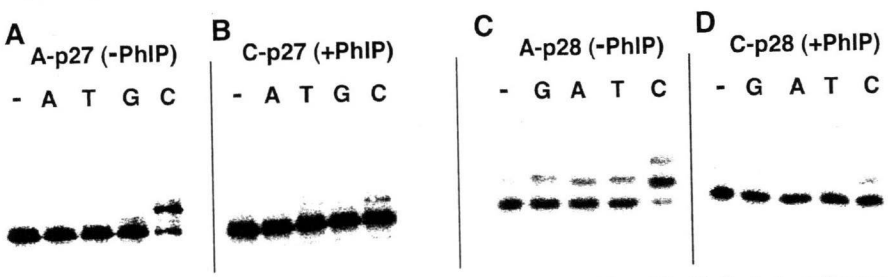

FIGURE 5. **Translesional DNA synthesis by pol η using substrates C-p27 and C-p28.** Control reactions were performed using substrates without the PhIP adduct, A-p27 (*A*) and A-p28 (*C*). An insertion reaction was performed with substrate C-p27 (*B*) and an extension reaction with substrate C-p28 (*D*). A single dNTP (G, A, T, C) was added into the reaction mixture as indicated by *G, A, T,* and *C above* each lane. The lanes indicated by − are controls without any nucleotides. Concentrations of pol η and each dNTP were 1.9 nM and 100 μM, respectively.

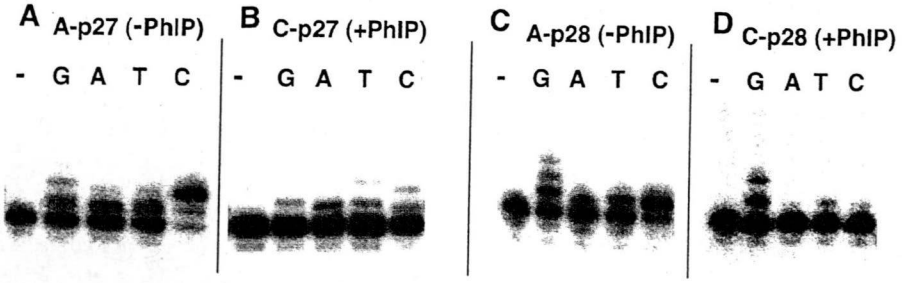

FIGURE 6. **Translesional DNA synthesis by pol κ using substrates C-p27 and C-p28.** Control reactions were performed using substrates without the PhIP adduct, A-p27 (*A*) and A-p28 (*C*). An insertion reaction was performed with substrate C-p27 (*B*) and an extension reaction with substrate C-p28 (*D*). A single dNTP (G, A, T, C) was added into the reaction mixture as indicated by *G, A, T,* and *C above* each lane. The lanes indicated by − are controls without any nucleotides. The concentrations of pol κ were 250 (*A* and *C*), 500 (*B*), and 1000 nM (*D*), respectively. The concentration of each dNTP was 100 μM.

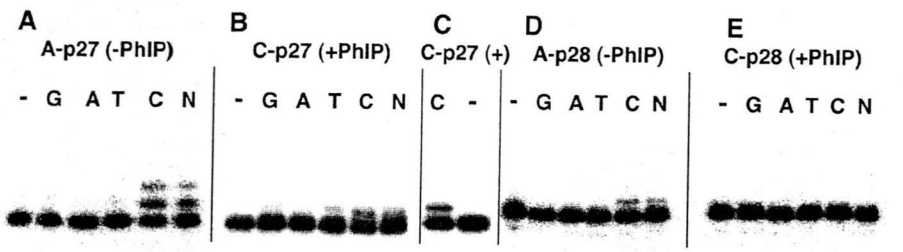

FIGURE 7. **Translesional DNA synthesis by REV1 using substrates C-p27 and C-p28.** Control reactions were performed using substrates without the PhIP adduct, A-p27 (*A*) and A-p28 (*D*). Insertion reactions were performed with substrate C-p27 (*B* and *C*) and an extension reaction with substrate C-p28 (*E*). A single dNTP (G, A, T, and C) or a mixture of each was added into the reaction mixture as indicated by *G, A, T, C,* and *N above* each lane. The lanes indicated by − are controls without any nucleotides. The concentrations of REV1 were 5.2 (*A* and *D*) and 26 nM (*B, C,* and *E*), respectively. The concentrations of each dNTP were 100 μM (*A, B, D,* and *E*) and 320 μM (*C*), respectively. The *N* mixture contained each dNTP at a concentration of 25 μM.

We next examined translesional DNA synthesis beyond the PhIP adduct using a truncated form of human DNA polymerase κ containing the N-terminal 559 amino acids. One or two dCs were inserted opposite the dG-C8-PhIP adduct by this polymerase, and misinsertions of three other nucleotides were also observed to a certain extent (Fig. 6*B*). pol κ incorporated two dCs and misincorporated dG, dA, and dT into the A-p27 substrate without the PhIP adduct at a low efficiency (Fig. 6*A*). Misincorporations of dG, dA, and dT into the A-p28 substrate without the adduct were also observed (Fig. 6*C*). In the case of the extension reaction from 3′-dC opposite the dG-PhIP adduct, pol κ also incorporated dC and misincorporated dT into the C-p28 substrate at low efficiency (Fig. 6*D*). Interestingly, one- and two-base incorporations of dG into the substrate C-p28 by pol κ dominated the incorporation of a dC (Fig. 6*D*). In the extension reaction with pol κ in the presence of all four dNTPs, fragments of 29 and 30 nucleotides were observed as major products, and a small amount of the 31-nucleotide fragment was observed (see supplemental Fig. S5, *lane 6*). Full-length products of 32 nucleotides were observed only when an excess amount of pol κ was present (data not shown). This poor extension activity of pol κ after adding two nucleotides was probably caused by the shortness (~4 nucleotides) of the 5′ region to the lesion in the template oligonucleotide. Extension with pol κ, pol η, and pol δ from the mismatched primers, where the 3′-terminal nucleotide of the p28 primer, dC, was substituted with another nucleotide, could not be observed (data not shown). REV1 inserted a dC opposite the PhIP adduct at a higher efficiency compared with pol κ and pol η (Fig. 7, *B* and *C*). REV1 was, however, unable to catalyze the extension reaction from the dC opposite the PhIP adduct in C-p28 (Fig. 7*E* and supplemental Fig. S5, *lane 5*). REV1 incorporated only dC nucleotides into A-p27 and A-p28 substrates without the adduct (Fig. 7, *A* and *D*). Neither nucleotide insertion nor extension reactions for the templates containing the PhIP adduct were detected using human pol ι (data not shown).

Kinetic Analyses of Translesional DNA Synthesis by pol κ and REV1—To evaluate translesional DNA synthesis beyond the dG-C8-PhIP adduct in further detail, additional quantitative analyses for pol κ and REV1 were performed. Insertion reactions catalyzed by pol κ for dC (Fig. 8, *B, lanes 2–5,* and *C, closed diamonds*) and dG (Fig. 8, *B, lanes 6–9,* and *C, closed triangles*) into substrate C-p28 were analyzed in the same way. Kinetic parameters for pol κ were determined using steady-state kinetic assays (Table 2). The catalytic efficiency (k_{cat}/K_m) of dC insertion into C-p28 (0.039 min^{-1} mM^{-1}) was found to be 4-fold greater than that into C-p27 (0.011 min^{-1} mM^{-1}). These results indicate that pol κ catalyzes the extension reaction from the 3′-terminal of dC opposite the dG-C8-PhIP with a higher efficiency than the insertion reaction opposite the adduct. The k_{cat}/K_m values of the dC insertion opposite the adduct were roughly 4 orders of magnitude less than those into counterparts without the adduct (see Table 2). The k_{cat}/K_m value of the dG incorporation into C-p28 was slightly higher than that of dC, and more than 8-fold higher than that of dG into C-p27 (see Table 2). This result indicates that pol κ skipped over the dG site just 5′ of dG-C8-PhIP on the template and incorporated dG opposite dC on the template strand of substrate C-p28 with a high efficiency. The k_{cat}/K_m values of the dC incorporation into D-p27 (0.19 min^{-1} mM^{-1}) were over 4-fold greater than into C-p28 (0.039 min^{-1} mM^{-1}) and over 8-fold higher than that of dG into B-p29 (0.023) (see supplemental Table S1). These data indicate that the efficiencies of the extension reaction by pol κ are the highest for template p32D containing the PhIP adduct in the third G of the triple G run, next for template p32C containing the PhIP/adduct in the second G, and lowest for template p32B containing the PhIP adduct in the first G.

Even at higher concentrations of dNTPs, extension reactions catalyzed by REV1 for substrate C-p28 could not be monitored (Table 3, Fig. 7*E*). The k_{cat}/K_m value of the dC incorporation by REV1 into substrate C-p27 was more than 2,000 times greater than that by pol k, and 1/44 of the values for counterparts with-

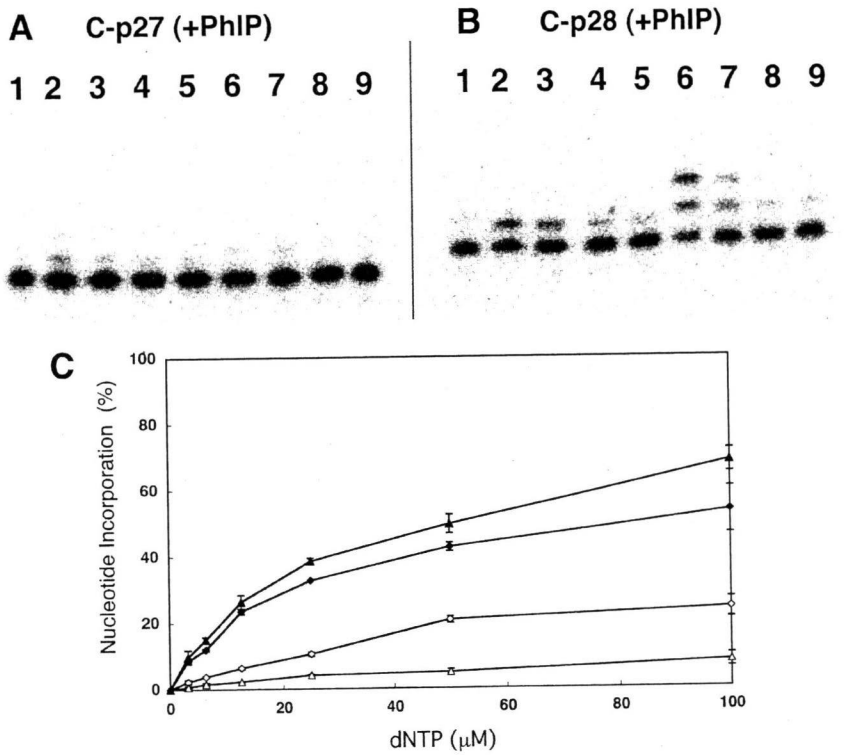

FIGURE 8. **Translesional DNA synthesis by pol κ.** Nucleotide incorporation by pol κ for substrates C-p27 (*A*) and C-p28 (*B*). Either dCTP (*lanes 2-5*) or dGTP (*lanes 6-9*) was added into the reaction mixture. *Lane 1* indicates a control without any nucleotides. The concentration of pol κ was 910 nM. The concentrations of dCTP or dGTP, respectively, were 25 (*lanes 2* and *6*), 12.5 (*lanes 3* and *7*), 6.25 (*lanes 4* and *8*), and 3.13 μM (*lanes 5* and *9*). *C*, incorporation efficiencies of dCTP and dGTP into substrate C-p27 and C-p28. Incorporations of dCTP into C-p27, dGTP into C-p27, dCTP into C-p28, and dGTP into C-p28 are indicated by *open diamonds*, *open triangles*, *closed diamonds*, and *closed triangles*, respectively. Each data point represents the mean of two separate experiments. The *error bars* represent residuals.

TABLE 2
k_{cat}/K_m values for pol κ

Substrate	K_m	k_{cat}	k_{cat}/K_m
	μM	$\times 10^{-3}$ min^{-1}	min^{-1} mM^{-1}
C-p27			
dCTP	70	0.76	0.011
dGTP	47	0.24	0.0050
C-p28			
dCTP	8.0	0.32	0.039
dGTP	11	0.48	0.042
A-p27			
dCTP	0.035	4.4	130
dGTP	0.26	1.3	5.0
A-p28			
dCTP	0.027	3.7	140
dGTP	2.1	8.8	4.1

TABLE 3
k_{cat}/K_m values for dCTP-insertion by REV1

Substrate	K_m	k_{cat}	k_{cat}/K_m
	μM	$\times 10^{-3}$ min^{-1}	min^{-1} mM^{-1}
C-p27	12	320	27
C-p28	ND[a]	ND	ND
A-p27	0.36	390	1100

[a] ND, not detectable.

out the adduct (Table 3). The k_{cat}/K_m values of the dC insertion by REV1 into three substrates, B-p28, C-p27 and D-p26, were 39, 27, and 73 min^{-1} mM^{-1}, respectively. Thus, the insertion reaction catalyzed by REV1 among the three templates was the most efficient for template p32D containing the PhIP adduct at the third G, similar to the extension reaction by pol κ.

DISCUSSION

In Vitro TLS Analysis Reconstituting PhIP-induced Mutations—HCAs are food-borne carcinogens produced when cooking meat (1, 9, 33). The most significant aspect of these molecules is that they exist normally in cooked food and are thus ubiquitous carcinogens (32). The mutagenicity and carcinogenicity of HCAs are mainly attributed to C8- and N2-dG adducts (9). Both excision repair and translesional DNA synthesis play critical roles in the mutagenesis steps induced by HCAs. However, despite the importance of HCAs as common environmental mutagens, there have been very few previous reports regarding the stalling of DNA polymerases and TLS caused by the DNA adducts they form. This is mainly because of the difficulty in preparing template DNA with introduced HCA adducts at specific sites. Choi *et al.* (34) have recently undertaken a biochemical study of TLS at adducts of the HCA 2-amino-3-methylimidazo[4,5-*f*]quinoline (IQ) using purified human polymerases. In our current study of TLS, we describe our findings for adducts of PhIP, the most abundant HCA in cooked foods (4).

A rat colon cancer model induced by PhIP shows profiles of cancer development similar to the multistep model of colon carcinogenesis in humans (35). In this rat model, *p53* and K-*ras* mutations are rarely observed, whereas mutations in *Apc* and its downstream gene *β-catenin* have been frequently observed (21, 36–38). Hence, mutations in *Apc* or *β-catenin* have been speculated to play a critical role in PhIP-induced colon carcinogenesis. Five mutations in the *Apc* gene were previously detected in four of eight PhIP-induced rat colon tumors, and all of these mutations involved a single guanine deletion in the 5′-GGGA-3′ sequence (21). This characteristic mutation induced by PhIP, 5′-GGGA-3′ to 5′-GGA-3′, was also observed in other *in vivo* mutation analyses using transgenic animals harboring introduced reporter genes, such as *lacI* (18–20). Hence, the 5′-TCCGGGAAC-3′ sequence corresponding to a mutation hot spot within the rat *Apc* gene, which we utilized to introduce the PhIP adduct and employed as the template for *in vitro* DNA synthesis analyses, could be a suitable model for revealing the molecular mechanisms associated with PhIP-induced mutations.